

Extended Modulation Bandwidth of DBR and External Cavity Lasers by Utilizing a Cavity Resonance for Equalization

Geert Morthier, *Member, IEEE*, Richard Schatz, and Olle Kjebon, *Member, IEEE*

Abstract—We have investigated the occurrence of a second resonance frequency in distributed Bragg reflector laser diodes and the high modulation bandwidth resulting from it. The influence of different laser parameters has been theoretically investigated. It is also shown that a similar behavior can be obtained in laser diodes with a passive, low-loss, and gratingless external cavity. The possibilities of large-signal digital modulation are also investigated.

Index Terms—DBR laser, direct modulation, external cavity, semiconductor laser diode.

I. INTRODUCTION

THE OCCURRENCE of second resonance frequencies in the modulation response of single-mode distributed Bragg reflector (DBR) laser diodes, resulting in very high 3-dB bandwidths, has been described previously and has been observed both experimentally and theoretically [1], [2]. It was attributed to a second mode that is spectrally close to the main mode, but is not lasing and acts as a catalyst. The effect is due to one of the optical modulation sidebands being resonantly amplified by the cavity. 3-dB bandwidths in excess of 70 GHz have been predicted (but not yet experimentally verified) for such lasers. The appearance of a second resonance and its possible use in obtaining high modulation bandwidths has previously also been investigated for push-pull modulated DFB laser diodes [3]. An experimental result illustrating this effect is shown in Fig. 1. The two-section DBR laser is from the same batch as the laser in [2], which showed similar behavior, although less pronounced. It has a 190- μm long active section and a 300- μm long, as-cleaved Bragg section (with coupling coefficient estimated at 80 cm^{-1}). The active layer consisted of 12 wells, 7-nm thick, with 1% compressive strain, separated by 8-nm thick strain compensated barriers, giving a large differential gain and a relatively large confinement factor.

The analysis in [1] was limited to DBR laser diodes with small coupling coefficient (e.g., 20 cm^{-1} or less), zero reflection at the facet of the Bragg section, and for lasing at frequencies below the Bragg frequency. In order to better understand the effect and its possible use for high bit rate communication,

Manuscript received March 17, 2000; revised July 19, 2000. This work was supported by the European Commission under TMR-project FALCON.

G. Morthier is with the Department of Information Technology, Ghent University - IMEC, B-9000 Gent, Belgium.

R. Schatz and O. Kjebon are with the Laboratory of Photonics and Microwave Engineering, Royal Institute of Technology, S-11640 Kista, Sweden.

Publisher Item Identifier S 0018-9197(00)10557-3.

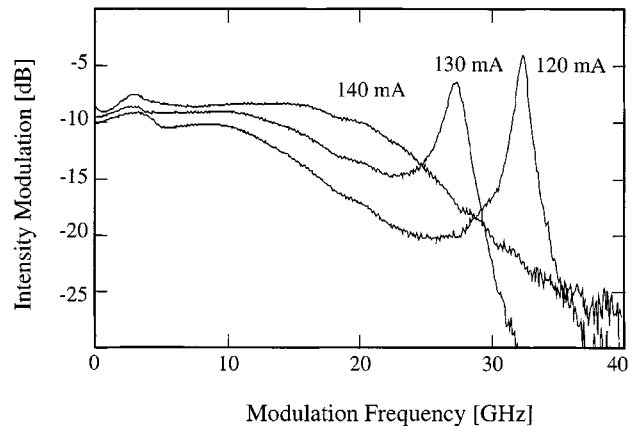


Fig. 1. Experimentally obtained modulation response for a two-section InGaAsP DBR laser emitting at 1.55 μm .

we have done a more thorough investigation and have considered a number of DBR laser diodes with different parameters.

The outline of the paper is as follows. In the next section, we investigate, through numerical simulation, the necessary conditions that have to be fulfilled in order for the second resonance to occur and the bandwidth to be enhanced. One of the findings is that it is essential to minimize the losses of the Bragg grating. We furthermore show numerically that it is not strictly necessary to have a side mode separated from the main mode by a frequency difference equal to the second resonance frequency in order to get a strong second resonance and a high modulation bandwidth. In fact, the second resonance can be explained more accurately as a compound cavity effect, which may or may not manifest itself in a true external cavity mode (i.e., for which the phase resonance condition is fulfilled).

In a third section of this paper, we show an example where the same behavior is obtained in laser diodes with a gratingless passive external cavity. For this case, we have also derived an analytical approximation for the small-signal modulation response from the Lang-Kobayashi equations. This analytical approximation is found to agree well with the numerical longitudinal model and can, for example, explain the numerically observed high modulation bandwidths.

In a fourth section, we briefly discuss some of the large-signal possibilities of the external cavity effect. It is well known that a certain small-signal bandwidth does not guarantee a similar bandwidth for on-off switching. A separate numerical analysis of the on-off switching possibilities of DBR lasers with high

small-signal bandwidth has, therefore, been performed. Direct on–off modulation at 40 Gb/s seems theoretically possible.

II. NUMERICAL RESULTS FOR DBR LASERS AND DISCUSSION

A second resonance peak occurs as soon as one of the optical modulation side-bands coincides with a cavity resonance. This can, in principle, happen in all laser diodes. However, in order for the second resonance to be visible in the modulation response and to significantly enhance the bandwidth, it has to be strong enough and at a moderate frequency distance from the normal modulation resonance related to the carrier-photon interaction. In other words, the first resonance peak should occur at rather high frequencies, and both the gain and frequency separation between main and side mode should be rather small. For the first resonance peak to occur at rather high frequencies, one in general has to consider short cavities and high bias currents. For the separation between main and side mode to be small, one has to consider long cavities. This contradiction can, however, be circumvented in DBR lasers, as will be further discussed below.

We have done a numerical analysis of the modulation response of a variety of DBR lasers, using the long-established laser diode model CLADISS [4]. In this model, a small-signal approximation of the single-mode longitudinal coupled-wave equations and the carrier-rate equations is used and the resulting linear equations are solved for a harmonic variation of the injected current. Important is that in this modeling, the propagation delays are taken into account since the modulation periods are no longer much larger than the cavity roundtrip times. The common parameters for all simulated DBR laser diodes are summarized in Table I. The laser diodes do not include a phase section and are composed of an active and a Bragg section only. The front facet is always taken as being cleaved, and the active section is assumed to be lossless. This last assumption implies that currents as well as relaxation resonance frequencies are a bit lower than what they would be if scattering losses in the active section were included.

A numerical IM-response for a two-section DBR laser, obtained at a bias current of 150 mA and showing a frequency dependence similar to the experimental result in Fig. 1, is given in Fig. 2. The DBR laser has a 120- μm long active section and a 700- μm long lossless Bragg section with a coupling coefficient $\kappa = 30 \text{ cm}^{-1}$, a zero internal loss, and an anti-reflection (AR) coated facet. The appearance of a second mode close to the main mode (separated by about 0.3 nm = 35 GHz) can be seen in Fig. 3, which shows the wavelength dependence of the roundtrip gain for the DBR laser diode considered in Fig. 2. The correlation between the side mode in Fig. 3 and the second resonance in Fig. 2 is obvious. The second resonance, however, is only strong if the first resonance frequency is sufficiently high, i.e., at high bias current.

For the laser diode of Figs. 2 and 3, the first resonance frequency is high (over 10 GHz) in spite of the rather large cavity length (820 μm). This high resonance frequency is due to the detuned loading [5], [6] (i.e., the increase of the losses with increasing wavelength), but also to the fact that the laser diode itself acts as a compound cavity. From the phase variation of the roundtrip gain in Fig. 3, one can clearly distinguish (for

TABLE I
COMMON DEVICE PARAMETERS OF THE DBR LASER DIODES

Parameter	Value
Active section length [μm]	120
Thickness of active layer [μm]	0.2
Width of active layer [μm]	2
Confinement factor	0.3
Monomolecular recombination coefficient [1/ns.]	1.4
Bimolecular recomb. coef. [cm^3/s]	10^{-10}
Auger recomb. coef. [cm^6/s]	$7.5 \cdot 10^{-29}$
Differential gain [cm^2]	$5 \cdot 10^{16}$
Transparency carrier density [cm^{-3}]	$1.15 \cdot 10^{18}$
Linewidth enhancement factor	5
Reflectivity l.h.s. facet	28%
Gain suppression [W^{-1}]	1.

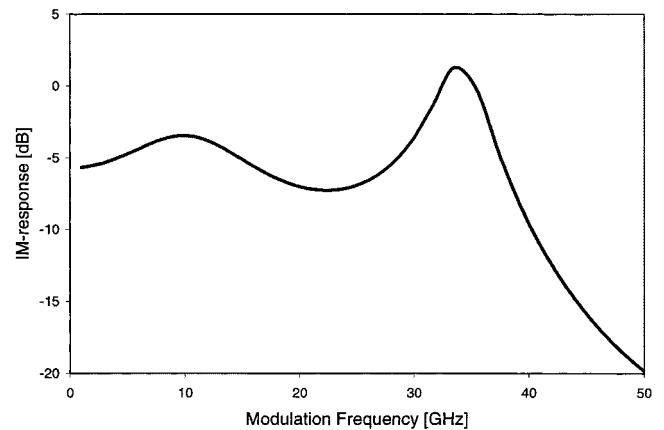


Fig. 2. Calculated intensity modulation response (at 150-mA bias current) of a DBR laser with AR-coated facet at the Bragg section and for $\kappa = 30 \text{ cm}^{-1}$ and $\alpha_{\text{int}} = 0 \text{ cm}^{-1}$.

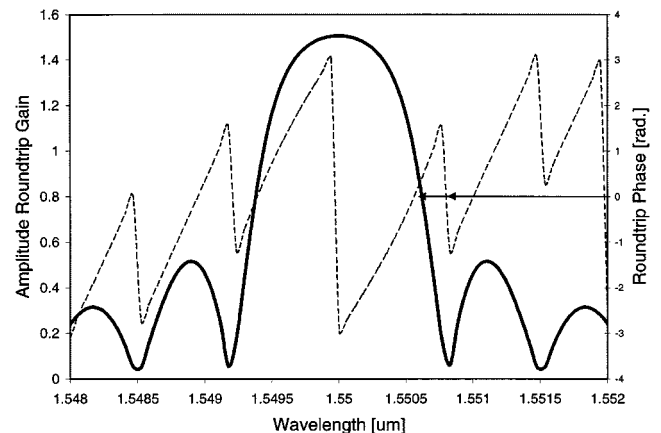


Fig. 3. Roundtrip gain versus wavelength for the DBR laser diode with AR-coated facet at the Bragg section and for $\kappa = 30 \text{ cm}^{-1}$ and $\alpha_{\text{int}} = 0 \text{ cm}^{-1}$. The lasing mode and the mode enhancing the modulation are indicated by arrows.

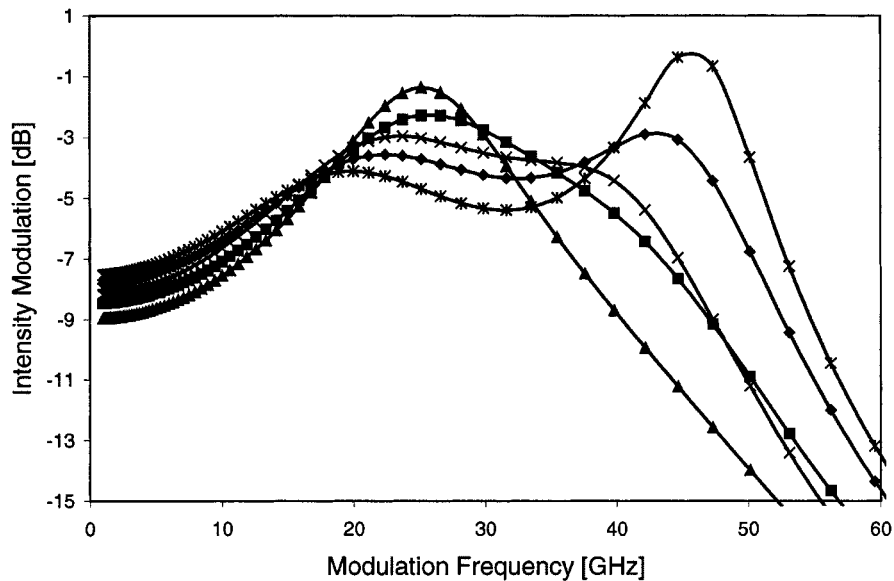


Fig. 4. Intensity modulation response (at 150 mA bias current) of the DBR laser with AR-coated facet at the Bragg section and $\kappa = 30 \text{ cm}^{-1}$ for $\alpha_{\text{int}} = 5$ (*), 10 (♦), 15 (×), 20 (■), and 25 (▲) cm^{-1} . (A grating phase of 190° was assumed).

example, from the average slope of the phase over a full $2\text{-}\pi$ variation, in the vicinity of the Bragg wavelength) that the fundamental mode spacing is around 1.6 nm, corresponding to an effective cavity length of around $200 \mu\text{m}$. That is, due to the distributed reflection, the Bragg section only has a penetration depth of around $80 \mu\text{m}$. The extra structure in the phase dependence is due to compound cavity modes, i.e., a significant part of the light penetrates much deeper into the Bragg section and sees an effective cavity length of around $800 \mu\text{m}$. It must be emphasized, though, that the Bragg section gives distributed reflections and an external cavity is perhaps just a mathematical equivalent. The rather large external cavity length causes the second resonance to occur at low frequency and, thus, to be strong.

It can be remarked that from the experimental results in Fig. 1, it appears that the second resonance frequency decreases with increasing bias current or, more precisely, that the second resonance frequency moves toward the first, becomes more damped, and finally merges with the first resonance frequency. This decrease of the second resonance frequency is presumably due to thermal effects and current leakage from the active into the Bragg section. Both effects can change the loss and the refractive index of the Bragg section significantly. In all simulations (which did not take into account thermal effects and current leakage), the second resonance frequency remained more or less constant as a function of the bias current.

A. Influence of Losses and Coupling Coefficient

For DBR laser diodes with an AR-coated Bragg section, we found that a second resonance can only enhance the modulation bandwidth if the internal absorption in the Bragg section is not too high (e.g., below 20 cm^{-1}). In that case, but only for specific values of the grating phase, one obtains a second mode (or quasimode) at rather small distance from the main mode.

As the internal losses in the Bragg section increase, the first resonance frequency increases, and there is more and

more overlap between first and second resonances. This is illustrated in Fig. 4, which shows the modulation response (at 150-mA bias current) of a DBR laser diode with a $500\text{-}\mu\text{m}$ long Bragg section with $\kappa = 30 \text{ cm}^{-1}$ for different values of the internal loss in the Bragg section. As the losses increase further, the distinction between both resonances disappears and one obtains a single (broad) resonance. Moreover, as the losses increase, the range of grating phases for which the extremely high modulation bandwidths can be obtained narrows.

The influence of the grating phases on the modulation response of the above laser is illustrated in Fig. 5. One can see a sudden change in response between the phases 166° and 167° . This corresponds to a mode jump. For a phase of 166° , the laser is lasing slightly on the short wavelength side of the Bragg wavelength and the first resonance frequency is rather small. For a phase of 167° , maximum detuned loading on the long wavelength side is obtained and a high first resonance frequency and very strong second resonance are the result. As the phase further increases, the detuned loading and the first resonance frequency slowly decrease and the second resonance slowly becomes weaker. However, as can be seen, a high bandwidth is obtained over a rather large range of grating phases for this laser.

The influence of the coupling coefficient is not easily illustrated. As the coupling coefficient changes, one has to assume different ranges for the grating phases to obtain two resonances in the modulation response. However, in general, the range of grating phases for which a high modulation bandwidth can be found narrows when the coupling coefficient increases and grating phases were not found anymore for, e.g., $\kappa = 100 \text{ cm}^{-1}$. An example was found, however, for $\kappa = 80 \text{ cm}^{-1}$ and for the case $\alpha_{\text{int}} = 10 \text{ cm}^{-1}$. The modulation response of this laser (with, again, a $500 \mu\text{m}$ long Bragg section) at a bias current of 150 mA is shown in Fig. 6. From the inset, showing the roundtrip gain spectrum, it can be seen that there is not really a side mode at 50 GHz from the main mode. There is only a slight decrease in the phase of the roundtrip gain and

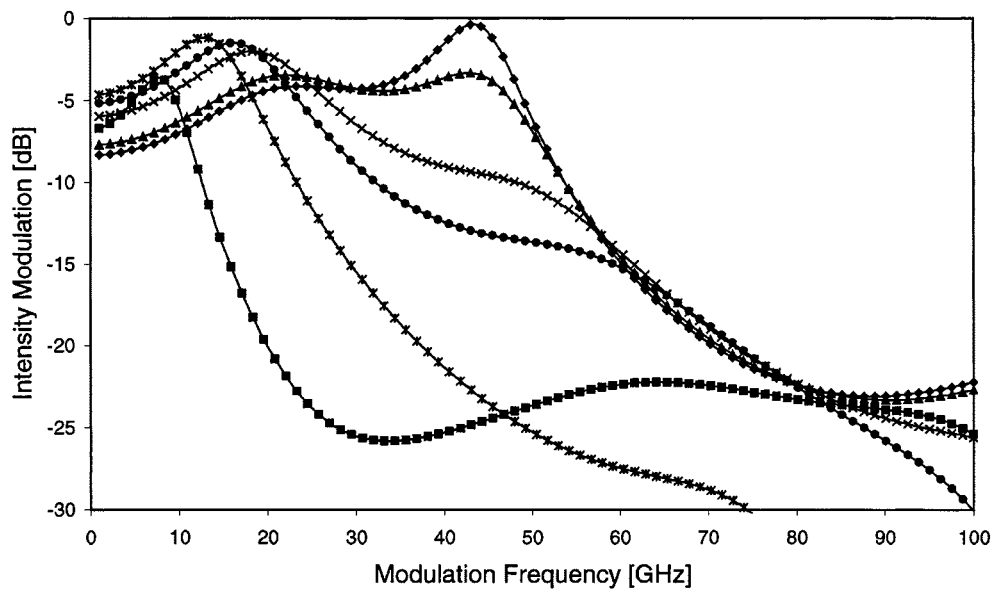


Fig. 5. Intensity modulation response (at 150 mA bias current) of a DBR laser with AR-coated facet at the Bragg section and $\kappa = 30 \text{ cm}^{-1}$ and $\alpha_{\text{int}} = 10 \text{ cm}^{-1}$ and for the grating phases $\phi_{\text{gr}} = 166^\circ$ (■), 167° (◆), 200° (▲), 300° (×), 0° (●), and 100° (*).

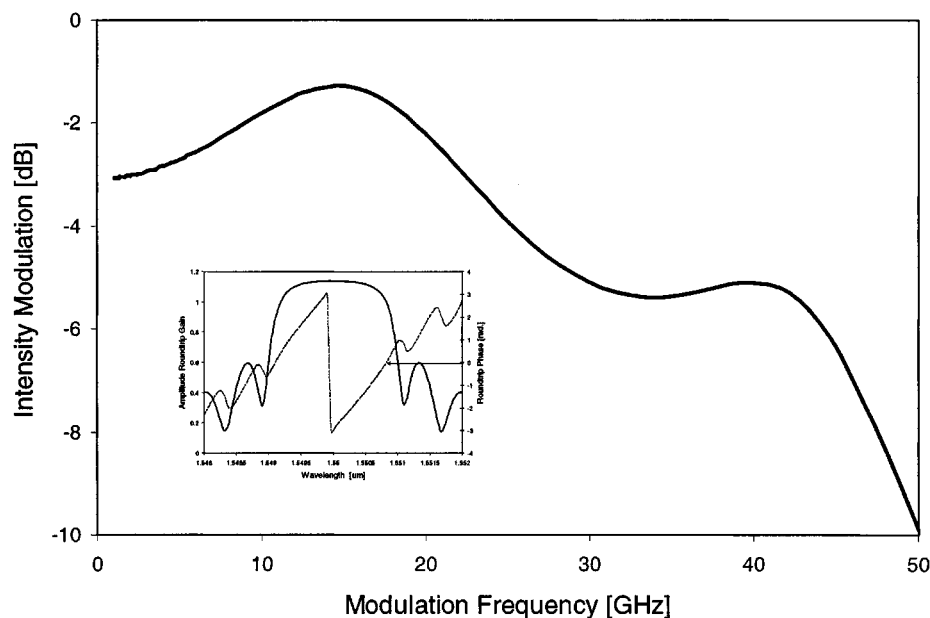


Fig. 6. Intensity modulation response (at 150 mA bias current) of a DBR laser with AR-coated facet at the Bragg section and for $\kappa = 80 \text{ cm}^{-1}$ and $\alpha_{\text{int}} = 10 \text{ cm}^{-1}$ (grating phase = 350°). The inset shows the wavelength dependence of the roundtrip gain corresponding with this laser (with again the arrow indicating the lasing mode).

a peak in the amplitude. Hence, it is not strictly necessary to have a side mode close to the main mode in order to get two resonances in the modulation response and, as a result, a high modulation bandwidth. Obviously, as the internal losses or the coupling coefficient in the Bragg section increase, an ever smaller portion of the light penetrates deep into the Bragg section and the compound cavity behavior of the DBR laser becomes weaker.

B. Influence of Bragg-Section End Reflection

When the Bragg section is cleaved, a similar behavior with similar dependencies on the laser parameters as for AR-coated Bragg-section facets can be obtained. In this case, however,

second resonances in the modulation response seem to be more common. This is not surprising since the reflection from the cleaved facet makes the external cavity effect stronger. In lasers with Bragg end reflection the second resonance was found to occur even for lasers emitting at the short wavelength side of the Bragg wavelength and/or for higher values of the internal absorption in the Bragg section. To demonstrate that the high modulation bandwidth is not only obtained if lasing is at the long wavelength side of the Bragg peak, we briefly discuss the case of a laser that emits on the short wavelength side of the Bragg wavelength. We consider a DBR laser for which the Bragg section has $L = 500 \text{ }\mu\text{m}$, $\kappa = 30 \text{ cm}^{-1}$, and $\alpha_{\text{int}} = 0 \text{ cm}^{-1}$, and a cleaved facet. The modulation response at a bias current of

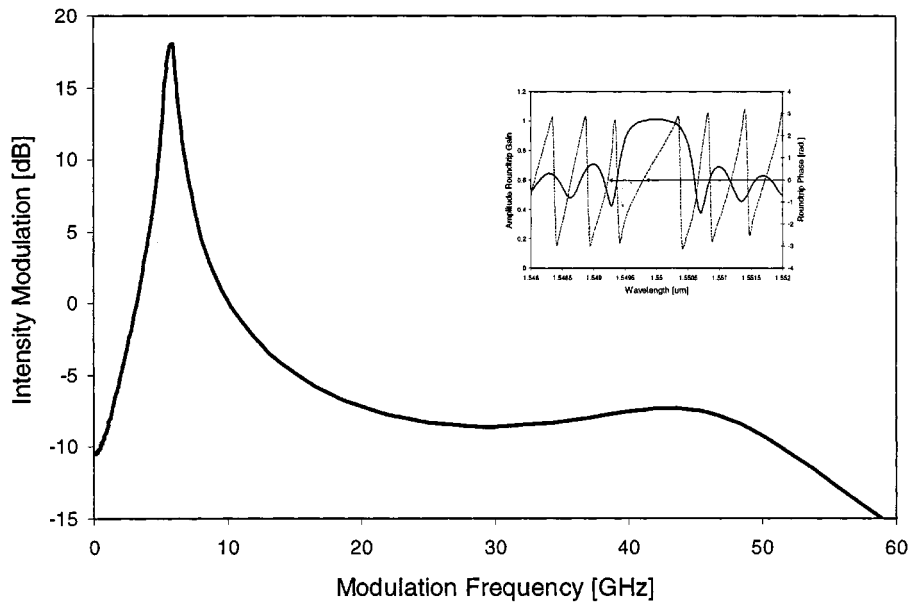


Fig. 7. Intensity modulation response (at 150-mA bias current) of a DBR laser with cleaved facet at the Bragg section and for $\kappa = 30 \text{ cm}^{-1}$ and $\alpha_{\text{int}} = 0 \text{ cm}^{-1}$ (grating phase = 264°). The inset shows the wavelength dependence of the roundtrip gain corresponding with this laser (lasing mode and modulation enhancing side mode are indicated by arrows). The grating phase is chosen such that lasing at the short wavelength side of the Bragg wavelength is obtained.

150 mA, with an inset showing the roundtrip gain spectrum, is shown in Fig. 7. As can be seen, the first resonance peak is little damped this time due to the specific detuning. However, again a 3-dB modulation bandwidth of over 50 GHz is obtained. It is important to remark that in this case the first resonance frequency is rather low (around 6 GHz). From the wavelength dependence of the phase of the roundtrip gain in this case, it can be concluded that now the DBR laser again acts as a single cavity. The losses and distributed reflection in the Bragg section are so small that most of the light reaches the facet adjacent to the Bragg grating where it is reflected back toward the gain section. The behavior as a single cavity with a rather large length of $620 \mu\text{m}$ is another reason why the first resonance frequency is small for this laser diode.

III. EXTERNAL CAVITY LASER DIODES

As has been pointed out in the previous section, the occurrence at rather low frequencies of a second resonance frequency in the modulation response of DBR laser diodes can be attributed to the compound or external cavity behavior of these laser diodes. In this section, we elaborate further on this idea. First, we can justify the external cavity behavior of the DBR laser diode further by showing the resemblance between the roundtrip gain spectra of the DBR laser diodes considered in the previous section, and of a real external cavity laser diode. The wavelength dependence of the roundtrip gain of such an external cavity laser diode (in fact, a DFB laser diode with length $120 \mu\text{m}$ and facet reflectivities of 5%, to which a lossless passive cavity of length $400 \mu\text{m}$ and with facet reflectivity of 1% is attached) is shown in Fig. 8. The phase variation exhibits similar structure as in the DBR laser diodes, while there is now also extra structure in the amplitude variation. This extra structure in the amplitude can, just as a detuned loading, be used to increase the frequency of the first resonance in the

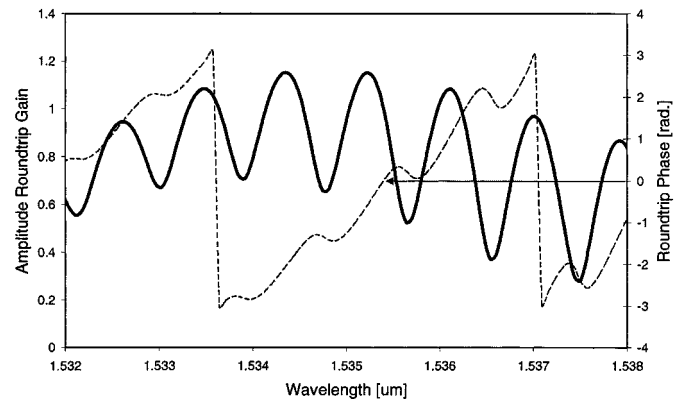


Fig. 8. Roundtrip gain versus wavelength for a DFB laser diode with 5% reflection at both facets ($\kappa L = 0.6$) to which a lossless passive $400\text{-}\mu\text{m}$ long cavity with 1% reflection is attached (the lasing mode is indicated by an arrow).

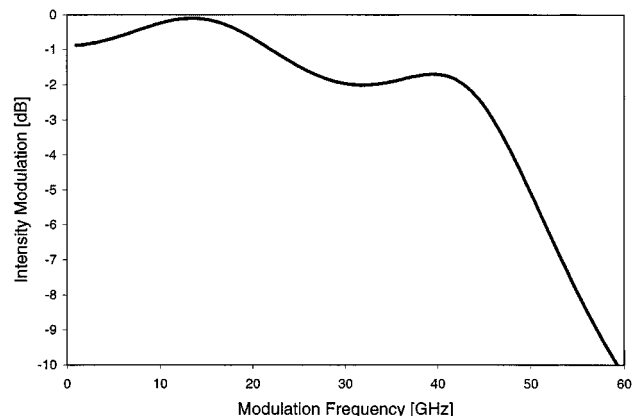


Fig. 9. Modulation response (normalized) obtained from the analytical expression for an output power of 50 mW and using the device parameters from Table I and $k_c = 10^{11} \text{ s}^{-1}$, $\tau = 0.025 \text{ ns}$.

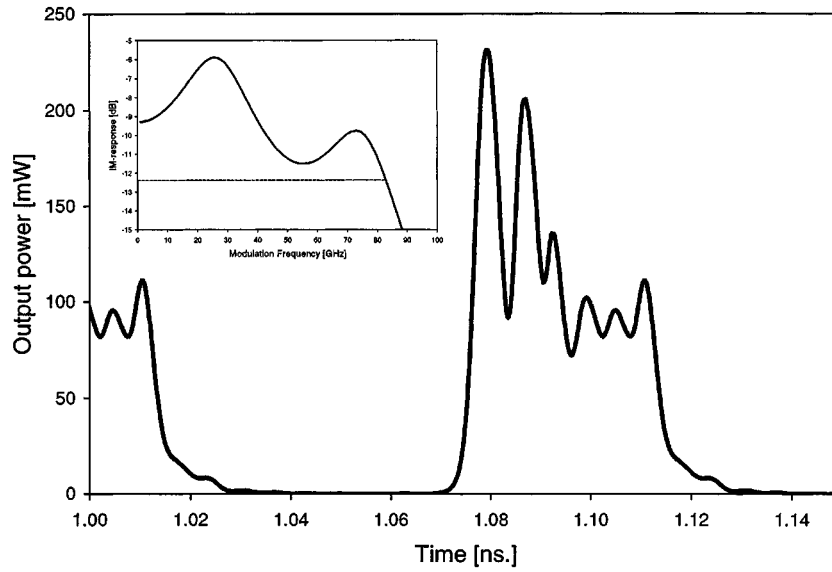


Fig. 10. Output power as a function of time of a DBR laser with 80-GHz small-signal bandwidth (cf. inset) and on-off modulated at 20 Gb/s.

modulation response. For this external cavity laser, numerical simulations have, indeed, confirmed that a similar modulation response as that shown in Figs. 4–6 is obtained.

For simple external cavity laser diodes, it is possible to derive the small-signal response analytically, starting from the Lang–Kobayashi equations [7]. For the photon density in the active section S and field phase φ

$$\frac{dS}{dt} = (G - \gamma)S + 2k_c \sqrt{S(t)S(t-\tau)} \cdot \cos(\omega_0\tau + \varphi(t) - \varphi(t-\tau)) \quad (1)$$

$$\begin{aligned} \frac{d\varphi}{dt} &= \Delta\omega \\ &= \frac{\alpha}{2} \frac{dG}{dN} \Delta N - k_c \sqrt{\frac{S(t-\tau)}{S(t)}} \\ &\quad \cdot \sin(\omega_0\tau + \varphi(t) - \varphi(t-\tau)) \end{aligned} \quad (2)$$

where τ is the delay time in the external cavity (determined by its length and refractive index), G is the modal gain ($1/s$), and γ is the modal loss. ω_0 can be taken as the pulsation of the steady-state field, in which case $\omega_0\tau = 2k\pi$. k_c is the feedback coefficient and is given by $(\tau_a)^{-1}(r_3/r_2)$, where τ_a is the roundtrip time in the active section, and r_2 and r_3 are the field reflections from the interface between active and passive waveguides and from the passive waveguide, respectively. From the time-dependent field equations (1) and (2), and the usual equation for the carrier density, one can derive the intensity modulation response. For the simple case of $\omega_0\tau = 2k\pi$, one finds (3), shown at the bottom of the page, where τ_d is the differential carrier lifetime and V is the volume of the active section. It can be

noticed that a different expression is given in [8]. The expression in [8] is for a single long cavity which is partly active and partly passive (and without reflection at the interface between both parts), whereas (3) is for a short cavity with a weak external, distant reflection (i.e., there is a reflection at the interface between the active and passive parts). For a laser with a threshold gain of $1.44 \cdot 10^{12} \text{ s}^{-1}$, an average internal power of 100 mW (which corresponds roughly with 50 mW of output power, if both laser facets are cleaved), $k_c = 10^{11} \text{ s}^{-1}$, $\tau = 0.025 \text{ ns}$, and other parameters as given in Table I, one obtains from expression (3) the modulation response shown in Fig. 9. The resemblance with Fig. 6 is remarkable. The analytical expression is interesting to optimizing laser designs for maximum modulation bandwidth

IV. SOME LARGE-SIGNAL AND CHIRP RESULTS

In order to get a very high 3-dB modulation bandwidth, we considered a two-section DBR laser with an $100\text{-}\mu\text{m}$ long active section and a $300\text{-}\mu\text{m}$ long lossless AR-coated Bragg section with a coupling coefficient of 40 cm^{-1} . The laser exhibited a threshold current of 6.2 mA and, at a bias current of 150 mA, a small-signal modulation bandwidth of over 80 GHz was obtained (see the inset of Fig. 10). The laser was then, at various bit rates, on-off modulated between 7 mA (corresponding to an output power of 1.1 mW) and 300 mA (corresponding to an output power of 90 mW). Fig. 10 shows the output power for periodic on-off modulation at a bit rate of 20 Gb/s, and in the inset, the small-signal response. The output power (unfiltered) exhibits an extinction ratio of over 20 dB. One can see that nice pulses are obtained with small rise and fall time. Fig. 11 shows

$$\frac{\Delta S}{\Delta I} = \frac{\frac{dG}{dN} \frac{S_0}{qV}}{\left[j\Omega + \frac{1}{\tau_d} + \frac{dG}{dN} S_0 \right] \left[j\Omega + k_c(1 - e^{-j\Omega\tau}) + \varepsilon G_{th} S_0 \right] + \frac{dG}{dN} G_{th} S_0} \quad (3)$$

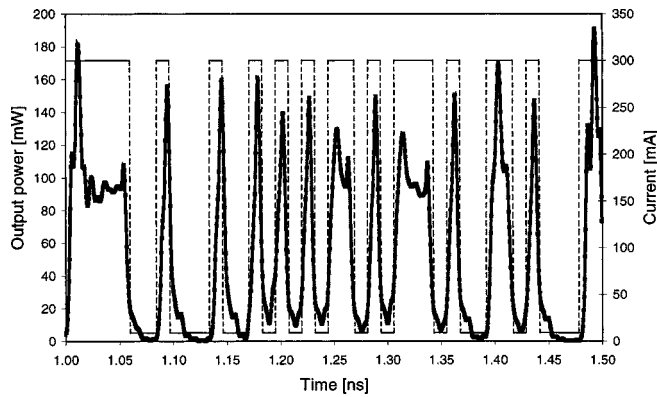


Fig. 11. Output power as a function of time of a DBR laser with an 80-GHz small-signal bandwidth for a PRBS signal at 80 Gb/s.

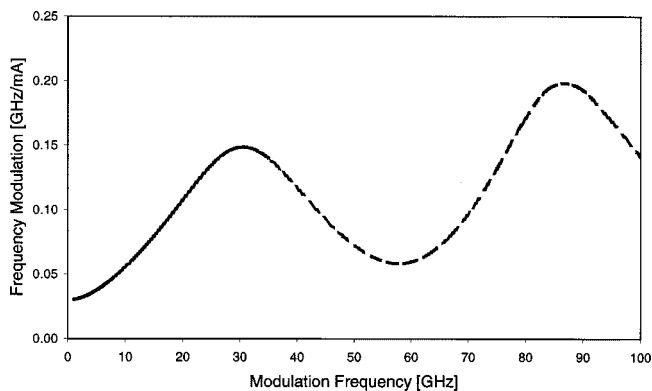


Fig. 12. FM response (in GHz/mA) of the laser of Fig. 9 at a bias current of 150 mA.

the output power for a pseudorandom bit sequence at 80 Gb/s. An extinction ratio of 10 dB is still obtained. A more severe problem at bit rates of 40 and 80 Gb/s is the timing jitter caused by different turn-on delays depending on the number of zeros preceding a one. This jitter implies that some coding is necessary and useful bit rates may therefore be limited to slightly smaller values than theoretically achievable.

Another important limitation at these ultrahigh bit rates is caused by the fiber dispersion. It is crucial that the laser does not exhibit excessive wavelength fluctuations, chirp, when modulated. The small-signal FM response at 150 mA of the laser in question is plotted in Fig. 12. Despite an assumed large value of five for the linewidth enhancement factor of the active layer material, the laser exhibits a remarkably low FM response of around 0.2 GHz/mA, even at ultrahigh modulation frequencies. This low chirp can be explained by the detuned loading effect, which suppresses carrier fluctuations in the laser cavity.

V. CONCLUSIONS

It has been shown theoretically that two-section DBR laser diodes can exhibit a modulation response with two strong resonances and, as a result, a 3-dB bandwidth of over 50 GHz under a variety of conditions. This kind of behavior has been demonstrated for a variety of values for the internal absorption and the coupling coefficient of the Bragg section, and for

both AR-coated and cleaved facets of this Bragg section. The behavior however only occurs for certain grating phases of the Bragg section, so that in practice, some sort of wavelength tuning (e.g., thermal) may be required before the predicted large-modulation bandwidths can be observed. In practice, one will also have to ensure that the internal loss and coupling coefficient in the Bragg section are not too large and that the differential gain is sufficiently large.

While this behavior has been described exclusively for two-section DBR laser diodes, there is no reason why it shouldn't be found also in three-section DBR laser diodes. The presence of a phase section would imply a reduced first resonance frequency, but also a reduced mode spacing and, therefore, a reduced second resonance frequency. This will reduce the 3-dB bandwidth slightly in the case of not too long phase sections, but the maximum bandwidth would still be high.

We have shown that a similar behavior can also be obtained with external cavity laser diodes under certain conditions. For these lasers, an analytical description has been derived which can be used to derive optimized designs with maximum modulation bandwidth.

In addition, a limited number of large signal, time domain simulations have been performed to get an idea of the large-signal, digital modulation possibilities using the DBR and external cavity lasers with large small-signal bandwidth. From first simulations, it appears that direct on-off modulation at bit rates as high as 40 Gb/s is theoretically possible. These simulations were done under the assumption that electronic parasitics and external circuitry are sufficiently broadband to allow a 40-Gb/s current injection modulation.

Finally, from our simulations, the high modulation bandwidths seem to occur only for high output power and bias current levels. In practice, one could, however, optimize the active layer material and the structures such that high bandwidths are obtained at lower bias currents.

REFERENCES

- [1] U. Feiste, "Optimization of modulation bandwidth in DBR lasers with detuned Bragg reflectors," *IEEE J. Quantum Electron.*, vol. 34, pp. 2371–2379, 1998.
- [2] O. Kjebon, R. Schatz, S. Lourudoss, S. Nilsson, B. Stålnacke, and L. Bäckbom, "Two-section InGaAsP DBR-lasers at 1.55 μm wavelength with 31 GHz direct modulation bandwidth," in *Proc. 9th Int. Conf. Indium Phosphide and Related Materials*, MA, 1997, pp. 665–668.
- [3] D. D. Marcenac, M. C. Nowell, and J. E. Carroll, "Theory of enhanced amplitude modulation bandwidth in push-pull modulated DFB Lasers," *IEEE Photon. Technol. Lett.*, vol. 6, pp. 1368–1371, 1994.
- [4] P. Vankwikelberge, G. Morthier, and R. Baets, "CLADISS—A longitudinal, multi-mode model for the analysis of the static, dynamic and Stochastic behavior of diode lasers with distributed feedback," *IEEE J. Quantum Electron.*, vol. 26, pp. 1728–1741, 1990.
- [5] O. Kjebon, R. Schatz, S. Lourudoss, S. Nilsson, B. Stålnacke, and L. Bäckbom, "30 GHz direct modulation bandwidth in detuned loaded InGaAsP DBR-lasers at 1.55 μm wavelength," *Electron. Lett.*, vol. 33, pp. 488–489, 1997.
- [6] K. Vahala and A. Yariv, "Detuned loading in coupled cavity semiconductor lasers—effect on quantum noise and dynamics," *Appl. Phys. Lett.*, vol. 45, pp. 501–503, 1984.
- [7] R. Lang and K. Kobayashi, "External optical feedback effects on semiconductor injection laser properties," *IEEE J. Quantum Electron.*, vol. 16, pp. 347–355, 1980.
- [8] R. Nagarajan, S. Levy, and J. E. Bowers, "Millimeter wave narrowband optical fiber links using external cavity semiconductor lasers," *J. Light-wave Technol.*, vol. 12, pp. 127–136, 1994.

- [9] S. A. Gurevich, V. B. Gorfinkel, G. E. Shtengel, and I. E. Chebunina, "High frequency modulation and short optical pulse generation from a laser diode with the gain governed by free carrier heating," in *Dig. 13th Int.. Semiconductor Laser Conf.*, Takamatsu, Japan, 1992, paper D-36.

Geert Morthier (M'93) received the degree in electrical engineering and the Ph.D. degree from the University of Gent, Gent, Belgium, in 1987 and 1991, respectively.

Since 1991, he has been a Member of Staff of Gent University—IMEC, Gent, Belgium. His main field of interest is in the modeling and characterization of optoelectronic components, for which he has authored or co-authored over 70 papers. He is also one of the two authors of the *Handbook of Distributed Feedback Laser* (Norwood, MA: Artech House, 1997). He has been active in many European RACE, ACTS, and COST projects, and was the Project Manager of the ACTS project ACTUAL on widely tunable laser diodes in 1998–2000.

Richard Schatz received the Ph.D. degree in photonics from the Laboratory of Photonics and Microwave Engineering, Royal Institute of Technology (KTH), Stockholm, Sweden, in 1995 .

Since 1987, he has conducted research in the field of semiconductor lasers at the Laboratory of Photonics and Microwave Engineering, KTH. He spent 1992 as a Visiting Scientist with AT&T Bell Laboratories, Murray Hill, NJ, working with design and simulation of low distortion lasers for CATV applications. His research is mainly focused on modeling and dynamic characterization of laser diodes, both edge emitters and VCSELs. He has been an active participant in COST 240 and is currently Vice Chairman of COST 268.

Olle Kjebon (M'92) was born in 1960 in Stockholm, Sweden. He received the M.Sc. degree in engineering physics from the University of Uppsala, Sweden, in 1987, and the Ph.D. degree from the Royal Institute of Technology (KTH), Stockholm, Sweden, in 1999.

From 1987 to 1993, he was with the Swedish Institute of Microelectronics, working with epitaxy (HVPE), processing, and measurements of lasers. In 1993, he joined KTH and continued his work on lasers for high-frequency modulation, with more emphasis on the design analysis and applications. He is currently a Senior Researcher with KTH. He has a vast experience of laser technology, from epitaxy to transmission experiments, and has authored/co-authored more than 40 papers and contributed substantially to the European projects Race 2069 UFOS and COST 240.